Geosci. Model Dev. Discuss., 8, 4737–4779, 2015
www.geosci-model-dev-discuss.net/8/4737/2015/
doi:10.5194/gmdd-8-4737-2015

Geoscientific Model Development Discussions

Accounting for anthropic energy flux of traffic in winter urban road surface temperature simulations with TEB model

A. Khalifa[1,2,5], **M. Marchetti**[2], **L. Bouilloud**[3], **E. Martin**[4], **M. Bues**[5], **and K. Chancibaut**[1]

[1]IFSTTAR, Centre de Nantes, route de Bouaye, CS4, 44344 Bouguenais CEDEX, France
[2]Cerema – DTer Est – LR Nancy, 71 rue de la grande haie, 54510 Tomblaine, France
[3]Météo France, Direction de la Production, 42 avenue G. Coriolis, 31057 Toulouse CEDEX, France
[4]CNRM-GAME (Météo-France, CNRS), Météo France, 42 avenue G. Coriolis, 31057 Toulouse CEDEX, France
[5]Université de Lorraine, UMR 7359-GeoRessources CNRS/UL/CREGU, ENSG, 54518 Vandoeuvre-lès-Nancy CEDEX, France

Received: 23 April 2015 – Accepted: 22 May 2015 – Published: 22 June 2015

Correspondence to: A. Khalifa (abderrahmen.khalifa@cerema.fr)

Published by Copernicus Publications on behalf of the European Geosciences Union.

Abstract

A forecast of the snowfall helps winter coordination operating services, reducing the cost of the maintenance actions, and the environmental impacts caused by an inappropriate use of de-icing. In order to determine the possible accumulation of snow on pavement, the forecast of the road surface temperature (RST) is mandatory. Physical numerical models provide such forecast, and do need an accurate description of the infrastructure along with meteorological parameters. The objective of this study was to build a reliable urban RST forecast with a detailed integration of traffic in the Town Energy Balance (TEB) numerical model for winter maintenance. The study first consisted in generating a physical and consistent description of traffic in the model with all the energy interactions, with two approaches to evaluate the traffic incidence on RST. Experiments were then conducted to measure the traffic effect on RST increase with respect to non circulated areas. These field data were then used for comparison with forecast provided by this traffic-implemented TEB version.

1 Introduction

During the winter period, precipitations could accumulate on pavement surface, with a specific danger in the case of snow and black ice since it reduces road grip and therefore impacts the road user's safety. One of the roles of maintenance services during winter is to ensure the network use, since France winter season for road services runs from the 15 October of a year till the 15 March of the next year. Their interventions are grouped under the term winter maintenance designed to reach optimal conditions of safety and of mobility. For years, winter operations services have become conscious of the environmental risks such as the extensive use of de-icers on road networks. Through training actions and standards productions, they began to sensitize infrastructure managers to control the amounts spread. Many studies are dedicated to the forecast of the road surface temperature (RST) (Shao and Lister, 1995; Sass, 1997;

GMDD
8, 4737–4779, 2015

Paumier and Arnal, 1998; Chapman et al., 2001; Crevier and Delage, 2001; Raatz and Niebrügge, 2002; Bouilloud, 2006; Bouilloud et al., 2010). A forecast of the snowfall and RST helps coordination of winter maintenance services, optimizing their costs, and the environmental impacts caused by an inappropriate use of de-icers. Considerable effort has been given to meteorological forecasting of these adverse weather conditions, particularly for road freezing conditions (Rayer, 1987; Takle, 1990; Borgen et al., 1992; Sass, 1992; Brown and Murphy, 1996). To forecast RST, winter maintenance operators rely on numerical models. Improvement of these models consisted in including a spatial component to incorporate the influence of both meteorological and geographical parameters. However, traffic has so far been a challenging parameter for its inclusion in RST forecast (Prusa et al., 2002). In the present study, we will be interested in taking into account traffic impact in the modelization of the RST. A short literature review on the thermal effect of the traffic will be presented to identify and to quantify these impacts. A model dedicated to urban configuration was chosen. The flux associated to the traffic was investigated in details for their introduction into this model. The modification in the energy balance caused by the vehicles was then evaluated. Compared with initial traffic implementation in the model, two different approaches were considered. A first one consisted in improving the evaluation of the heat flux released by the traffic. The second one was based on an explicit representation of traffic into the model. Forecast and field results will be compared and discussed.

2 State of the art and objective of the study

Accumulation of snow or ice on roads generates hazardous traffic conditions. Several models deal with meteorological forecasting (Rayer, 1987; Sass, 1992; Shao and Lister, 1996; Chapman et al., 2001; Bouilloud, 2006; Bouilloud et al., 2010). These models did not or partially include heat associated with passing vehicles. Recently several researches were undertaken to study the thermal effects of traffic on the RST. A vehicle is a source of multiple forms of heat (Fig. 1) (Prusa et al., 2002). Indeed,

GMDD
8, 4737–4779, 2015

we can distinguish between direct and indirect consequences due to the passing vehicles on the road. Direct impacts are created by the heat flux generated by the engine and the exhaust system, the radiative flux emitted by the bottom of vehicle and the tire frictional heat flux. The vehicles also indirectly influence the road surface energy balance by the modification of the radiative balance. They can block long-wave radiation exchange whilst also preventing short-wave radiation from reaching the road surface during the day. Traffic motion will also cause additional mixing of air above the road surface promoting increased turbulent flow. Farmer and Tonkinson (1989) showed that the general cumulative effect of these impacts on the diurnal temperature cycle is to promote warmer RST on heavily trafficked roads. As an example, in a study in the Stockholm area (Sweden), Gustavsson and Bogren (1991) showed RST differences by up to 2 °C due to the differences in traffic conditions between urban and rural area, especially during peak hours. Surgue et al. (1983) reported that recorded RST were usually several degrees greater in the road where traffic is the heaviest. The impact of vehicles can be quantified on multi-laned roads, where the increased volume of slow vehicles on nearside lanes can increase RST of up to 2 °C (Parmenter and Thornes, 1986). Chapman et al. (2001) showed that traffic could cause up to 2 °C difference between inside and outside the highways and that the identification of traffic impacts on RST is relatively difficult. Moreover, they showed that the traffic effect depends on the traffic density, vehicle velocity, topographic profile of the road and atmospheric stability. Fujimoto et al. (2008) showed that the temperature in the vehicle-passage area was approximately 3 °C above the one in the non-vehicle-passage area during a sunny winter day. Furthermore, Fujimoto et al. (2010) reported that the RST under vehicles waiting at traffic signals was 3 to 4 °C higher than that nearby. Some experiments with a thermal mapping vehicle indicated traffic has a significant effect on RST (Khalifa et al., 2014), especially in traffic lights areas and/or on roads with high traffic density.

All the references quoted before are related to the winter season and shows that the traffic has a significant effect on the RST, especially near traffic signals and/or on the roads with high density of traffic. Our study aimed at describing this traffic effect during

GMDD
8, 4737–4779, 2015

the winter season on the pavement energy balance. It consisted in integrating the theoretical traffic description into TEB numerical model dedicated to urban configuration to numerically quantify how much the traffic energy input affects the RST and on the basis of field experimental measurements and data (weather, traffic).

3 The Town Energy Balance (TEB) model and the introduction of the fluxes associated to the traffic

3.1 The Town Energy Balance model

The TEB model consists in a parameterization adapted to the specific physical processes established in the urban atmospheric layer. It was developed by (Masson, 2000; Masson et al., 2013) in order to simulate the turbulent fluxes for urban areas. TEB model was originally developed for applications in meteorology and weather prediction at kilometer spatial scales, or at higher resolution. A previous work was performed to use TEB in a specific winter context (Pigeon et al., 2008), with a simple description of the traffic effect on the street atmosphere: the corresponding heat flux is added as a source term in the urban canyon. In the study presented here, an analysis is conducted on the possible ways to take into account traffic impact in the modeling of the RST in the winter season on the basis of Prusa and Fujimoto approaches (Prusa et al., 2002; Fujimoto et al., 2006, 2007, 2012).

The physical processes involved to modeling the road surface energy balance by the TEB model are summarized in Fig. 2. In this configuration, the road surface energy balance is expressed by the following equation:

$$\rho_{\text{road}} c_{\text{road}} \frac{\partial \text{RST}}{\partial t} \Delta Z_{\text{s}} = R_{\text{n}} + S_{\text{a}} + L + G \quad (1)$$

ΔZ_{s} is the thickness of the first layer of the road surface. We choose a very low thickness value (ΔZ_{s} equal to 0.001 m) so that its temperature reflects RST. ρ_{road} c_{road} is

GMDD
8, 4737–4779, 2015

the volumetric heat capacity of the road surface layer ($J\,m^{-3}\,K^{-1}$), t is the time (s), G is the conductive heat flux across the bottom of the road surface layer (pavement heat flux, $W\,m^{-2}$), R_n is the net radiation flux ($W\,m^{-2}$), S_a is the sensible heat flux associated with natural wind ($W\,m^{-2}$) and L is the latent heat flux associated with evaporation or condensation ($W\,m^{-2}$).

Figure 2 also shows the radiative interaction coefficients $LW_{x\_to\_y}$ between the various components x and y (sun, road, walls, garden, snow) of the urban canyon. These coefficients define the rate of radiative and energy exchanges between the various components of urban canyon. They are defined by the following equations:

$$LW_{Road\_to\_Sun} = \sigma\epsilon_{road}\,SVF_{road} + \epsilon_{road}(1-\epsilon_{walls})\,SVF_{walls}(1-SVF_{road}) \quad (2)$$

$$LW_{Road\_to\_Road} = \sigma\epsilon_{road}\left[\epsilon_{road}(1-\epsilon_{walls})(1-SVF_{road})\;SVF_{walls} - 1\right] \quad (3)$$

$$LW_{Snow\_to\_Road} = \sigma\epsilon_{road}(1-\epsilon_{walls})\,\epsilon_{snow}(1-SVF_{road})\;SVF_{walls} \quad (4)$$

$$LW_{Walls\_to\_Road} = \sigma\epsilon_{road}\,\epsilon_{walls}(1-SVF_{road})(1+(1-\epsilon_{walls}))(1-2SVF_{walls}) \quad (5)$$

$$LW_{Garden\_to\_Road} = \sigma\epsilon_{road}(1-\epsilon_{walls})\,\epsilon_{garden}(1-SVF_{road})\;SVF_{walls} \quad (6)$$

$LW_{Road\_to\_Sun}$ is the interaction radiative coefficient between road and sun, $LW_{Road\_to\_Road}$ is the one between road and road, $LW_{Snow\_to\_Road}$ between the snow layer and road, $LW_{Walls\_to\_Road}$ between walls and road and $LW_{Garden\_to\_Road}$ between garden and road. σ is the Stefan–Boltzmann constant ($5.67\times10^{-8}\,W\,m^{-2}\,K^{-4}$), ϵ_{road}, ϵ_{wall}, ϵ_{snow} and ϵ_{garden} are respectively the emissivity of the road (0.95), walls (0.90), snow layer (1) and garden (0.98). SVF_{road} and SVF_{walls} are respectively the sky view factors of the road and walls. These sky view factors are calculated by the TEB model on the basis of building height and on the road width of the urban canyon.

Among the interactions coefficients mentioned above, the one between snow and road only occurs in the presence of snow on the road. However, at this stage, the pavement was considered cleared of snow. Therefore this coefficient will not be taken into account in the calculation that follows. The interactions coefficients involved in the

GMDD
8, 4737–4779, 2015

calculation of net radiation at the road surface are described by the following equation.

$$R_n = R_{nl} + R_{ns} \quad (7)$$

$$R_{nl} = R_{ld} + R_{lu} \quad (8)$$

$$R_{ns} = R_{sd} + R_{su} \quad (9)$$

R_{nl} ($W\,m^{-2}$) and R_{ns} ($W\,m^{-2}$) are respectively the net of long and short wave radiation received by the road surface. R_{ld} ($W\,m^{-2}$) is the downward long wave radiation, R_{lu} ($W\,m^{-2}$) is the long wave upward radiation, R_{sd} ($W\,m^{-2}$) is the downward short wave radiation and R_{su} ($W\,m^{-2}$) is the upward short wave radiation.

Figure 2 also shows the aerodynamic resistance of the road R_{road}, used in the calculation of the turbulent sensible and latent heat flux S_a ($W\,m^{-2}$) and L ($W\,m^{-2}$) respectively defined in the TEB model by the following equations.

$$S_a = \frac{\rho_{air} c_p}{R_{road}}(RST - T_{lowcan}) = \rho_{air} AC_{road}(RST - T_{lowcan}) \quad (10)$$

$$L = \frac{\rho_{air} L_v}{R_{road\text{-}watt}}(Q_{sat\_road} - Q_{canyon}) = \rho_{air} AC_{road\text{-}watt}(Q_{sat\_road} - Q_{canyon}) \quad (11)$$

c_p is the specific heat capacity ($J\,kg^{-1}\,K^{-1}$), ρ_{air} is the air density ($kg\,m^{-3}$), RST the road surface temperature (K), T_{lowcan} is the temperature of the lower limit layer of urban canyon (K), and thus corresponds to the air temperature at 2 m high. L_v is the latent heat of liquid water evaporation ($J\,kg^{-1}$) Q_{sat_road} is the specific humidity in the road surface ($g\,kg^{-1}$), Q_{canyon} is the specific air humidity ($g\,kg^{-1}$), R_{road} is the aerodynamic resistance of a dry road, R_{road_wat} is the aerodynamic resistance of a wet road, and AC_{road}, AC_{road_wat} are the aerodynamic conductance's respectively for dry and wet road.

The conduction heat flow (G) between the first two road surface layers is calculated through the following equation using RST (first layer) and RST_2, temperature of the

GMDD
8, 4737–4779, 2015

second layer.

$$G_{1-2} = \lambda_1 \frac{\mathrm{RST} - \mathrm{RST}_2}{\frac{d_1+d_2}{2}} \quad (12)$$

λ_1 ($\mathrm{W\,m^{-1}\,K^{-1}}$) is the thermal conductivity of the first road layer, RST its temperature (K), RST_2 is the temperature of the second road layer (K), d_1 is the thickness of the first road layer (0.001 m, as mentioned before) and d_2 the one of the second road layer (0.01 m).

In this configuration of TEB, the traffic heat flux is involved in the calculation of the sensible $Q_{\mathrm{H\_TOP}}$ ($\mathrm{W\,m^{-2}}$) and latent turbulent heat flux $Q_{\mathrm{E\_TOP}}$ ($\mathrm{W\,m^{-2}}$) of the urban canyon. They are respectively represented by the following equations:

$$Q_{\mathrm{H\_TOP}} = Q_{\mathrm{H\text{-}ROAD}} + 2\frac{h}{w}Q_{\mathrm{H\text{-}WALL}} + \frac{1}{f_{\mathrm{road}}}Q_{\mathrm{H\text{-}TRAFFIC}} \quad (13)$$

$$Q_{\mathrm{E\_TOP}} = Q_{\mathrm{E\text{-}ROAD}} + \frac{1}{f_{\mathrm{road}}}Q_{\mathrm{E\text{-}TRAFFIC}} \quad (14)$$

$Q_{\mathrm{H\_TOP}}$ and $Q_{\mathrm{E\_TOP}}$ represent the fluxes at 2 m high above the urban canyon. h is the representative height building of urban canyon in the TEB model (m), w is its width (m). $1/f_{\mathrm{road}}$ represents the fraction of the road relative to the width of urban canyon. $Q_{\mathrm{H\_TRAFFIC}}$, $Q_{\mathrm{E\_TRAFFIC}}$ respectively represent the sensible and latent heat generated by traffic ($\mathrm{W\,m^{-2}}$). The values that were assigned to these two parameters are $Q_{\mathrm{E\_traffic}} = 0\,\mathrm{W\,m^{-2}}$ and $Q_{\mathrm{H\_traffic}} = 20\,\mathrm{W\,m^{-2}}$. The turbulent flow of urban canyon interacts with the road surface energy balance through the interactions radiative coefficient ($\mathrm{LW}_{x\_\mathrm{to}\_y}$) defined previously.

Bibliographic quoted above in the state of the art section indicated that traffic has a significant effect on RST. Our interest is then to integrate traffic parameters in modeling the road surface energy balance and to evaluate the energy inputs of traffic on RST. To do so, two approaches were then considered.

GMDD
8, 4737–4779, 2015

3.2 Improving the evaluation of the heat flux released by the traffic (first approach)

This first approach is based on the paramterization already introduced in TEB by Pigeon et al. (2008). The influence of the traffic is represented by the traffic sensible and latent heat fluxes ($Q_{H\_traffic}$ and $Q_{E\_traffic}$ in Fig. 2. In this study, a constant flow was considered and was added to the turbulent heat flux of urban canyon (Eqs. 13 and 14). This configuration was not adapted to a specific RST forecast. Indeed, the traffic energy input is not only involved in calculating the total heat flux generated by urban canyon, but it also affects the road energy balance. Furthermore, this heat input is not constant and depends on the traffic characteristics (volume, vehicle velocity and the daily distribution density).

The improvement provided by this first approach is to have the traffic heat input variable according to urban traffic characteristics (volume, vehicle velocity and density). The greater the traffic, the lower the speed, then the larger its energy input. Therefore, the heat flux generated by the traffic would no longer be considered as a constant throughout the whole period of the simulation. In addition, this approach allows us to test the TEB model sensitivity to the variation of the traffic heat inputs.

The energy provided by the traffic has been studied by several authors (Klysik, 1996; Ichinose et al., 1999; Sailor and Lu, 2004; Pigeon et al., 2007, 2008; Colombert, 2008). The global heat flux generated by a vehicle, named Q_v, can be expressed as a function of the net heat combustion (NHC), the fuel density ϱ_{fuel} and its average consumption FE as follows:

$$Q_v = \frac{\mathrm{NHC}\ \rho_{fuel}}{\mathrm{FE}} \tag{15}$$

According to Guibet (Guibet, 1998), the NHC ($\mathrm{J\,kg^{-1}}$) is equal to 42 700 for gasoline and 42 600 for diesel. The fuel density ϱ_{fuel} ($\mathrm{kg\,L^{-1}}$) is equal 0.775 for gasoline and 0.845 for diesel. The average fuel consumption FE ($\mathrm{km\,L^{-1}}$) depends on the type of fuel and on the type of traffic. In the study made by Colombert (Colombert, 2008), FE is of the

GMDD
8, 4737–4779, 2015

order of 8.5 km L^{-1} (this includes among others over-consumption due to air conditioning: 3.1 L 100 km^{-1} for gasoline cars in urban cycle and 3.2 L 100 km^{-1} for diesel ones). According to the values from the literature (Sailor and Lu, 2004; Pigeon et al., 2007; Colombert, 2008), an average Q_v value of 3903 J per vehicle travel distance was selected, which corresponds to an energy per second for a given average vehicle speed. Inspired by the formula defined by Sailor and Lu (2004), the instantaneous flux of heat generated by traffic can be evaluated by the following equation:

$$Q_{traffic}(t) = \frac{1}{S_{impact}} \frac{1}{V_{veh}} D_{veh}(t) Q_v \quad (16)$$

D_{Veh} is the traffic density (vehicles s^{-1}), V_{veh} is the vehicles velocity ($m\,s^{-1}$), S_{impact} is the traffic area impact. In this configuration, the S_{impact} will be considered equal to the width of the street canyon ($S_{impct} = W_{canyon} = 10$ m). Q_v is the global heat flux from a vehicle ($J\,s^{-1}$). Based on the Eq. (16) and considering traffic data in a given street of Nancy (France), where the study was conducted, the traffic heat contribution $Q_{traffic}$ to the energy balance varies with time. It increases with the traffic volume and is weak during the off-peak hours when the traffic density is low. This is illustrated in Fig. 3. To introduce the energy provided by the traffic in the TEB model, we should distinguish between the sensible and latent heats. Based on the estimation from Pigeon et al. (2007), $Q_{traffic}$ was then partitioned into sensible and latent heats, respectively represented by the following equation:

$$Q_{H\text{-}traffic}(t) = 0.92\, Q_{traffic}(t) \quad (17)$$

$$Q_{E\text{-}traffic}(t) = 0.08\, Q_{traffic}(t) \quad (18)$$

3.3 Explicit representation of traffic into the model (second approach)

This approach is based on a detailed study of the various processes of traffic impacts, and a parameterization of the physical equations that describe each process of traffic impact were performed. The tire friction heat S_t in an extended temperature range,

GMDD
8, 4737–4779, 2015

the shield effect on radiative flux received by pavement surface from the environment and the radiative flux from the vehicle (R_v, $F_{IR\_veh\_inf}$, $F_{IR\_veh\_sup}$), the turbulent flux generated by passing vehicles, the sensible and latent heats released by the engine and exhaust system (E_{ex}, S_m) and the aerodynamic drag associated with the vehicle's movement were selected. A presentation of equations modified to take into account these processes in the TEB model was carried out and fully described in a previous paper (Khalifa et al., 2014), based on research papers from many authors (Jacobs and Raatz, 1996; Chapman et al., 2001; Prusa et al., 2002; Sato et al., 2004; Takahashi et al., 2005; Fujimoto et al., 2006, 2007, 2008, 2010, 2012), and is illustrated in Fig. 4a. The heat fluxes generated by the traffic considerably varies depending on the traffic condition (bolting, fluid circulation, urban context or highway, etc.) and traffic parameters (velocity, density, volume). Furthermore, the shielding due to vehicles on the road and the impact zone of their associated physical processes is partial. Khalifa et al. (2014) have identified an impact factor for each traffic physical process to evaluate its contribution, as indicated in Fig. 4b and Table 2. The parameters chosen for the description are the road width W_{road}, the vehicle length L_{veh}, and width W_{veh}, the ones of the impact area of the engine respectively L_m and W_m, the ones of the impact area of the tires respectively L_p and W_p, and the radius of the impact area of the exhaust system R_{ex}. Based on traffic data from the Charles III street (Nancy–France), the magnitude of the corresponding shield effect coefficient C_{shield} on the radiative flux of the road surface is shown in Fig. 3.

This second approach of traffic integration in the TEB model based in the resolution of tow surface energy balances. For the area not-impacted by passing vehicles, the energy balance corresponded to the initial TEB configuration. However, in the area impacted by the traffic, the physical processes of traffic were substituted the road surface parameters. Then, to modeling will be based on an average of RST of these road surface balances, therefore depending on $Z_{traffic}$, a constant between 0 and 1. It represents the percentage of the road impacted by the vehicle passage (Fig. 4c).

GMDD
8, 4737–4779, 2015

To integrate traffic with a simple and a relevant way in the TEB model, some assumptions were made. First, the heat flux generated by the engine S_m, the exhaust system E_{ex} and the flow of forced convection S_{va} generated by the passing vehicles are added to the urban canyon Q_{H_TOP} and Q_{E_TOP}. Then, the heat friction flux S_t is added to the road surface energy balance. This energy contribution is taken into account in the most appropriate location of the urban canyon, along with its interaction with flux of other components (road, walls). Concerning the radiative flux, the infrared radiation flux emitted by the vehicle is added to the infrared radiative flux received by the road surface. The infrared flux emitted by the bottom of the vehicle $F_{IR\_veh\_inf}$ is added to the long wave radiation flux received by the road surface R_{ld}, and the infrared flux emitted by the upper part of the vehicle $F_{IR\_veh\_sup}$ is added to the long wavelength flux of the atmosphere R_{lu}. The shield effect caused by the passing vehicles will decrease the radiative flux of the road surface. Based on these assumptions, the road surface energy balance is written in the following form:

$$\rho_{road} c_{road} \frac{\partial \mathrm{RST}}{\partial t} \Delta Z_s = (1 - Z_{traffic})(R_n + S_a + L + G) + Z_{traffic}(R_n^* + S_a^* + L^* + G + 0.22 C_{shield} S_t) \quad (19)$$

The (*) symbol denotes surface parameters impacted by traffic. The constant 0.22 represent the impact factor defined by Khalifa et al. (2014) for the tire frictional processes (Table 2). The net radiation impact on traffic R_n^* is expressed by the following equations:

$$R_n^* = R_{nl}^* + R_{ns} \quad (20)$$

$$R_{nl}^* = R_{ld}^* + R_{lu}^* \quad (21)$$

$$R_{ld}^* = (1 - C_{shield}) R_{ld} + (1 + C_{shield}) R_{IR\_veh\_inf} \quad (22)$$

$$R_{lu}^* = (1 - C_{shield}) R_{lu} + (1 + C_{shield}) R_{IR\_veh\_sup} \quad (23)$$

GMDD
8, 4737–4779, 2015

The sensible S_a^* (W m^{-2}) and latent L^* (W m^{-2}) heats in the presence of traffic on the road are respectively written:

$$S_a^* = \rho_{air} AC^*_{road} (RST - T_{lowcan}) \quad (24)$$

$$L^* = \rho_{air} AC^*_{road\text{-}watt} (Q_{sat\_road} - Q_{canyon}) \quad (25)$$

According the first hypothesis of integration of traffic impacts, the heat flows through the engine and the exhaust system are added to the turbulent heat flux of urban canyon, which influences the road surface energy balance. This is reflected by means of the following equations:

$$Q_{H\_TOP} = Q_{H\text{-}ROAD} + 2\frac{h}{w} Q_{H\text{-}WALL} + C_{shield} \frac{1}{f_{road}} Q_{H\text{-}TRAFFIC} \quad (26)$$

$$Q_{H\_TRAFFIC} = 0.25 S_m + 0.21 S_{ex} + S_{va} \quad (27)$$

The constants 0.25 and 0.21 represent the impact factor defined by Khalifa et al. (2014) respectively for the engine and the exhaust system (Table 2). An exhaustive list of abbreviations is provided in appendix, giving the all terms used in equations for both this article and the one of Khalifa et al. (2014).

4 Experimental measurements of traffic effect on urban RST

To identify the most appropriate approach to implement the traffic in TEB, some experiments were conducted. They consisted in RST measurements on pavement zones submitted and not submitted to traffic. The experimental zone was located in Charles III street (Nancy–France), having a canyon configuration consistent with TEB, with a width around 12 m (Fig. 5).

GMDD
8, 4737–4779, 2015

4.1 Description of the experiments, meteorological and traffic data

RST and atmospheric measurements were obtained using a vehicle parked in the selected street with a whole data acquisition on its board (Fig. 6a). Instruments first consisted in devices dedicated to meteorological parameters (T_{air}, relative humidity, wind direction and speed). They were installed on the roof of the vehicle, and data collected every 2 s. A radiometer and an infrared camera were respectively dedicated to RST without and with traffic. The radiometer was installed in a compartment at a controlled temperature, attached to the front bumper of the car, with measurements every 2 s too. The infrared camera was installed in a compartment on the vehicle roof. Thermal images of the pavement submitted to traffic were taken every 60 s. An illustration of instruments is given in Fig. 6b. Traffic data for the selected street was obtained from the appropriate service in Nancy.

Two experiments were then conducted. They consisted in continuously monitoring all parameters described above over a period of up to 48 h on the same locations and on two distinct dates, and with a variety of weather situations corresponding to an upcoming winter.

4.2 Weather and urban data inputs for TEB

Meteorological data used as forcing input for the TEB surface model come from the Nancy weather station located 2800 m away from the measurement site. Measurements available and used from this station are the air temperature at 2 m height (°C), air relative humidity at a height of 2 m (%), wind speed at a height of 10 m ($m\,s^{-1}$), direct and diffuse solar radiation ($W\,m^{-2}$), rain and snow precipitation (mm) and air pressure (Pa). These data cover both measurements campaigns with an hourly time step. The first campaign started on 20 November 2014 at 4 a.m. (LT) and lasted 48 h, and the second campaign was initiated on 17 December 2014 at 11 a.m. and lasted 30 h. Besides these meteorological parameters, the TEB scheme requires a parameterization of the coatings constituting the built urban area, such as the percentage of built area,

GMDD
8, 4737–4779, 2015

the height of buildings, the road width, the number of components layers of each urban surface covered (roof, walls and road), their thickness, and their thermal characteristic (thermal conductivity and heat capacity). The selected elements were the one initially present in the TEB urban data input, and considered as consistent with the buildings configuration of the experimental site. Some of them are provided in Table 3.

5 Results and discussion

5.1 Experimental results

The first step in our experimental study is to assess the magnitude of the traffic impact on the road surface temperature. Figure 7 indicates the RST of an area without traffic and the one submitted to traffic. It is noted that outside peak hours between 8 p.m. and 6 a.m. RST curves merge for the two zones. This reflects the reduced traffic flux input. However, during the day, we found that RST of the area submitted to traffic is greater by 1 to 3 °C with respect to the non-circulated one. The higher the traffic (especially during peak hours), the larger the gap between the two RST. The preliminary result of this experimental study confirms the ones reported in the literature (Gustavsson et al., 2001; Fujimoto et al., 2008). Firstly the RST differences do not only exist between a urban configuration and a rural one. The RST is also greater in a zone submitted to traffic with respect to another one traffic-free. This was observed in a full urban configuration. There is a clear relationship between hourly variation of thermal traffic contribution (Fig. 3) and hourly RST variation too.

The TEB model simulates an average RST. It does not distinguish between an area impacted by passing vehicles and other one without traffic. So as to compare the results provided by the TEB model with field data, we calculated a weighted average RST. In the following text, the measured road surface temperature RST_measured

GMDD
8, 4737–4779, 2015

corresponds to this weighted average RST according to the following relationship:

$$\mathrm{RST}_{\mathrm{measured}} = \frac{1}{\sigma\epsilon_{\mathrm{road}}}\left[\sqrt[4]{\frac{1}{3}\left(\sigma\epsilon_{\mathrm{road}}T^4_{\mathrm{Without\_traffic}}\right) + \frac{2}{3}\left(\sigma\epsilon_{\mathrm{road}}T^4_{\mathrm{With\_traffic}}\right)}\right] \quad (28)$$

The constants 1/3 and 2/3 respectively correspond to the portion of the road without traffic and the one submitted to traffic. These values are consistent with the numerical description of the second approach, respectively $1 - Z_{\mathrm{traffic}}$ and Z_{traffic}. Therefore, in the text that follows, the results of TEB model on RST will be compared to RST_measured. Its variations with time for the first experiment are illustrated in Fig. 7.

5.2 Comparison between RST from TEB in its initial configuration andfield data

As indicated above, in the initial configuration of the TEB model, traffic heat flux was already introduced. It was considered as a constant flux that is added to the heat flux of urban canyon. Figure 8 a provides a comparison between the RST simulated by the TEB model via the initial configuration of traffic (RST_TEB_IC) and RST_measured. There is an offset of 3 to 4 °C, RST_measured being greater than the RST_TEB_IC. This initial configuration does not properly take into account this traffic heat flux. This offset can be explained either by an improper traffic heat values input, or by inadequate traffic integration in the TEB model. Increasing $Q_{\mathrm{H\_traffic}}$ up to 200 $\mathrm{W\,m^{-2}}$ was not enough to reach a coincidence between RST_measured and RST_TEB_IC curves, the offset remaining of nearly 2 °C (Fig. 8b and c). Furthermore, the traffic peaks are not as visible as on field measurements, nor is the relationship with Q_{traffic} (Fig. 3). The RST increase is not as important as expected due to Q_{traffic} increase during peak hours. Nevertheless, this initial parameterization of traffic into the TEB model was not meant for RST forecast but more for global heat flux balance of a urban canyon (Pigeon et al., 2008).

GMDD
8, 4737–4779, 2015

5.3 Traffic integration results with the first approach

The constants of the traffic heat input set out in the initial configuration of traffic in TEB were not adapted with respect to flux generated by the traffic and indicated in the literature for RST forecast (Sailor and Lu, 2004; Pigeon et al., 2007, 2008; Colombert, 2008). The first approach consists in introducing a more accurate heat flux generated by vehicles, and then in testing the sensitivity of the road energy balance to its variation. Figures 8a illustrates the variations with time of RST_measured, RST_TEB_IC and the RST simulated according to the first approach (RST_TEB_A1) in the case of the first experiment.

The integration of traffic in the TEB model according to this first approach leads to a slight improvement in RST forecast. However, this improvement did not manage to reach values as observed on field data. Additional calculations were then conducted to evaluate to which extent the value of the heat flux generated by the traffic could be adjusted to obtain the best RST forecast. Values up to 200 $\mathrm{W\,m^{-2}}$ were then considered and results are plotted in Fig. 8b. They show none of the values was enough to obtain the experimental results. Indeed, such $Q_{\mathrm{H\_TRAFFIC}}$ values not only does not improve the modeling of the RST, but also they disrupt the Tair modeling, as illustrated in Fig. 8c. While taking into account the heat flux generated by the traffic according to the initial configuration value of $Q_{\mathrm{H\_TRAFFIC}} = 20\,\mathrm{W\,m^{-2}}$ gave T_{air} results consistent with the measurements, the allocation of larger values ($Q_{\mathrm{H\_TRAFFIC}} = 50$, 100, 150, and 200 $\mathrm{W\,m^{-2}}$) induce disruption in corresponding T_{air}. The results of Fig. 8c also justifies the purpose for which the traffic was integrated into the TEB model. In fact, the heat flux generated by the traffic was included under this initial configuration for the modeling of the overall heat flow in the urban canyon, this to assess this specific impact of anthropogenic heat flux on the urban comfort. This initial configuration of traffic in the TEB model can be valid according to the objective for which was taken into account, but it does not meet to the objective of our study about the evaluation of the traffic thermal impacts on the

GMDD
8, 4737–4779, 2015

RST modeling. This method should be modified to better take into account the traffic heat inputs, especially in winter conditions.

The study of the thermal mapping of traffic impacts carried out by Khalifa et al. (2014) indicated that the maximum effect of traffic is generated by the tire friction and the sensible heat flux exchanged between the vehicle and the road surface. It also indicates that the maximum traffic effect occurs in the immediate vicinity of the vehicle, approximately located 0.5 m from the ground. Indeed, in the TEB model, the urban canyon heat flux interacts at the first level of TEB located at 2 m height from the ground. Therefore, this integration of traffic as a source of heat in the urban canyon is not suitable. This description of the first approach can also be valid in the case of a global appreciation of anthropogenic flux.

5.4 Traffic integration results with the second approach

5.4.1 Results analysis

Traffic integration results using this approach are illustrated in Fig. 9. It compares the variation with time of RST for the different traffic integrations in the TEB model with RST from the first and the second experiments. RST results with the second approach (RST_TEB_A2) are closer to the field data than the one previously presented. The difference between field and calculated RST is of nearly 0.5 °C in average. RST variations reflect the ones of Q_{traffic} (Fig. 3) and their amplitudes (3 °C, Fig. 9a; 6 °C, Fig. 9b) are consistent with field measurements. RST_TEB_A2 profile indicates that this approach more properly took into account the heat inputs generated by traffic. We also found the peaks of heat inputs of traffic during rush hours were obtained with better agreement with respect to field measurements.

Analysis of the RST_TEB_A2 shows that RST forecast is improved by 2 to 3 °C with respect to RST_TEB_IC. This improvement primarily reflects the impacts of traffic on the RST and also that the configuration with which the traffic was introduced into the TEB model seems more appropriate for the case of winter season.

GMDD
8, 4737–4779, 2015

5.4.2 Model sensitivity

As indicated before, TEB model provides an average RST and does not distinguish between an area submitted to traffic and another one not.

The parameter $Z_{traffic}$ was integrated in the model to take into account the portion of the road affected by traffic. The sensitivity test of the TEB model to this parameter $Z_{traffic}$, was conducted. $Z_{traffic} = 1$ corresponds to the measurements undertaken by the infrared camera (RST_With_traffic). Figure 10 indicates that the results given by the TEB model (RST_TEB_A2 ($Z_{traffic} = 1$)) are close to RST_With_traffic. This confirms that the physical description of the traffic impacts process is suitable to the traffic integration in the TEB model for the winter season.

In urban areas, besides meteorological parameters, RST is also influenced by buildings configuration (percentage of buildings, building heights, widths of roads, type of materials used, etc. ...). Specific configurations where buildings are everywhere present in an urban environment, or fully absent, though not applicable in all urban, were tested to evaluate the sensitivity of the TEB model to this parameter. The results are shown in Fig. 11. It is found that without building the RST decreases from 0.5 °C, especially at night. This can be explained by the nature of building materials that store heat during the day and restores it at the night along with the absence of the radiative well created by buildings. In the absence of buildings, heat transfer phenomenon is absent.

A third validation of this approach based on an explicit representation of traffic on the model was conducted. It consisted in comparing air temperature measured onto the vehicle in the street and the forecast one obtained with TEB. Air temperature measurements are obtained at a height (1.8 m) and conditions (generation of a continuous laminar air flow on the probe) compliant with the one at which TEB is providing its results (2 m). Results are presented in Fig. 12. They indicated a good agreement between the forecast and the measurement in both experiments cases.

GMDD
8, 4737–4779, 2015

6 Conclusions

An experimental study was conducted to quantify the anthropic energy flux of traffic impact on RST in the winter season. It indicated an RST increase by 1 to 3 °C with respect to the absence of traffic. An additional work was undertaken so as to evaluate to which extent an accurate description of traffic might improve TEB numerical model when dedicated to RST simulations. Two approaches of traffic integration in this model were detailed and tested.

The integration of traffic in the TEB model according to the first approach and based on a variable heat flux into the canyon with time did not improve RST forecast. This approach can be used to evaluate the global anthropogenic heat flux in urban canyon, and is not meant for RST urban simulation. The results of the second approach, consisting in an accurate description of energy contributions of the traffic, were consistent with the experimental study as well as with the literature review. They indicated that the traffic increased RST by 1 to 3 °C and this increase depends on traffic conditions (vehicle velocity, traffic density and traffic impact area). Some TEB model sensitivity tests showed that traffic impact area affects the RST forecast. If this area is large, the thermal traffic flows are important which results in an increase of the RST. The presence or the absence of buildings also influenced the modeling of RST. A validation was also successfully obtained with the air temperature. To obtain a better forecast of the RST with the TEB model it is necessary to properly define the configuration of the urban environment. It should be noted that the integration of traffic in the TEB model according to this second approach significantly improved the RST forecast in the winter season. However, there is still a difference of 0.5 to 1 °C between the measurements and the TEB simulated RST. It can be explained either by the error that can be assigned to the measurement devices, or because the physical description we have used for the process of traffic impacts still needs improvements, or by the existence of some road parameters that have not yet been introduced into the RST forecast with the this model.

GMDD
8, 4737–4779, 2015

In the same context that this studies, other work is in progress to study the sensitivity of the TEB model to different physical processes of traffic. The objective of this work is to assess the contribution of each of the traffic impact process in improving the RST modeling TSR according to traffic parameters and the variation of the atmospheric stability.

These thermal impacts of traffic should also be coupled with the road surface water balance of the TEB model to assess the influence of the presence of water in its various forms (water, ice and snow) on the RST modeling.

Acknowledgements. Authors would like to take this opportunity to thank IFSTTAR and Météo France for their financial support, and Mathieu Moutton and Stéphane Ludwig for performing all measurements.

References

Bouilloud, L. and Martin, E.: A coupled model to simulate snow behavior on roads, J. Appl. Meteorol. Clim., 45, 500–516, 2006. 4739

Bouilloud, L., Martin, E., Habets, F., Boone, A., Le Moigne, Livet, P. J., Marchetti, M., Foidart, A., Franchistéguy, L., Morel, S., Noilhan, J., and Pettré, P.: Road surface condition forecasting in France, J. Appl. Meteorol. Clim., 48, 2513–2527, 2010. 4739

Brown, B. G. and Murphy, A. H.: Improving forecasting performance by combining forecasts: the example of road surface temperature forecasts, Meteorol. Appl., 3, 257–265, 1996. 4739

Browne, A. L., Wicker, D., and Segalman, D.: A general model for power loss in pneumatic tires, GM Research Laboratories, GMR-4005, Engineering Mechanics Department, 1980.

Borgen, J., Gustavsson, T., and Londquist, S.: A description of a local climatological model used to predict temperature variation along stretches of road, Meteorol. Mag., 121, 157–165, 1992. 4739

Chapman, L., Thornes, J. E., and Bradley, A. V.: Modeling of road surface temperatures from a geographical parameter database. Part 1: Statistical, Meteorol. Appl., 8, 409–419, 2001. 4739, 4740, 4747

GMDD

8, 4737–4779, 2015

Colombert, M.: Contribution to the analysis of the various means to take into account urban climate in urban planning, PhD thesis, Engineering Science, University of Paris-Est, France, 2008. 4745, 4746, 4753

Crevier, L. P. and Delage, Y.: METRo: a new model for road-condition forecasting in Canada, J. Appl. Meteorol., 40, 2026–2037, 2001. 4739

Farmer, S. F. and Tonkinson, P. J.: Road Surface Temperature Model Verification Using Input Data from Airfields, Roadside Sites and the Meso-Scale Model, UK Meteorological Office, Exeter, UK, 1989. 4740

Fujimoto, A., Watanabe, H., and Fukuhara, T.: Effects of tire frictional heat on snow covered road surface, in: Proceedings of the 13th SIRWEC Conference, Torino, Italy, 25–27 March, 6 pp., available at: http://www.sirwec.org/Papers/torino/17.pdf (last access: 22 May 2015), 2006. 4741, 4747

Fujimoto, A., Watanabe, H., and Fukuhara, T.: Modeling of vehicle heats and its influence on surface temperature of dry road, Doboku Gakkai Ronbunshuu E, 63, 202–213, 2007. 4741, 4747

Fujimoto, A., Watanabe, H., and Fukuhara, T.: Effects of vehicle heat on road surface temperature of dry condition, in: Proceedings of the 14th Standing International Road Weather Conference, Standing International Road Weather Commission, Prague, Czech Republic, ID05, available at: http://www.sirwec.org/Papers/prague/5.pdf (last access: 16 April 2015), 2008. 4740, 4747, 4751

Fujimoto, A., Saida, A., Fukuhara, T., and Futagami, T.: Heat transfer analysis on road surface temperature near a traffic light, Proceedings of the 17th ITS World Congress, Busan, South Korea, Intelligent Transportation Society, T_AP01138, 2010. 4740, 4747

Fujimoto, A., Watanabe, H., and Fukuhara, T.: A new approach to modeling vehicle-induced heat and its thermal effects on road surface temperature, J. Appl. Meteorol. Clim., 51, 1980–1993, 2012. 4741, 4747

Guibet, J. C.: Carburant liquides, Techniques de l'ingénieur, BE 8545, 1998. 4745

Gustavsson, T. and Bogren, J.: Infrared thermography in applied road climatological studies, Int. J. Remote Sens., 19, 1311–1328, 1991. 4740

Gustavsson, T., Bogren, J., and Greeb, C.: Road climate in cities: a study of Stockholm area, south-east Sweden, Meteorol. Appl., 8, 481–490, 2001. 4751

Ichinose, T., Shimodozono, K., and Hanaki, K.: Impact of anthropogenic heat on urban climate in Tokyo, Atmos. Environ., 33, 3897–3909, 1999. 4745

GMDD
8, 4737–4779, 2015

Ishikawa, N., Narita, H., and Kajiya, H.: Contribution of heat from traffic vehicle to snow melting on roads, Transp. Res. Record, 1672, 28–33, 1999.
Jacobs, W. and Raatz, W. E.: Forecasting road surface temperature for specific site characteristics using an energy balance model, in: Proceeding of the 8th SIRWEC Conference, Birmingham, UK, 17–19 April, 10 pp., 1996. 4747
Khalifa, A., Marchetti, M., and Buès, M.: Appreciation of the traffic effects on the RST by infrared thermography, SPIE Proc. Ser., 9223, 92230F, doi:10.1117/12.2061791, 2014. 4740, 4747, 4749, 4754, 4762
Klysik, K.: Spatial and seasonal distribution of anthropogenic heat emissions in Lodz, Poland, Atmos. Environ., 30, 3397–3404, 1996. 4745
Masson, V.: A physically-based scheme for the urban energy budget in atmospheric models, Bound.-Lay. Meteorol., 94, 357–397, 2000. 4741
Masson, V., Le Moigne, P., Martin, E., Faroux, S., Alias, A., Alkama, R., Belamari, S., Barbu, A., Boone, A., Bouyssel, F., Brousseau, P., Brun, E., Calvet, J.-C., Carrer, D., Decharme, B., Delire, C., Donier, S., Essaouini, K., Gibelin, A.-L., Giordani, H., Habets, F., Jidane, M., Kerdraon, G., Kourzeneva, E., Lafaysse, M., Lafont, S., Lebeaupin Brossier, C., Lemonsu, A., Mahfouf, J.-F., Marguinaud, P., Mokhtari, M., Morin, S., Pigeon, G., Salgado, R., Seity, Y., Taillefer, F., Tanguy, G., Tulet, P., Vincendon, B., Vionnet, V., and Voldoire, A.: The SURFEXv7.2 land and ocean surface platform for coupled or offline simulation of earth surface variables and fluxes, Geosci. Model Dev., 6, 929–960, doi:10.5194/gmd-6-929-2013, 2013. 4741
Parmenter, B. S. and Thornes, J. E.: The use of a computer model to predict the formation of ice on road surfaces, Research Report, 71, Transport and Road Research Laboratory, 1–19, 1986. 4740
Paumier, J. L. and Arnal, M.: Expérimentation Préviroute sur l'autoroute A75 dans le Cantal, Revue Générale des Routes et des Aérodromes, 758, 44–51, 1998. 4739
Pigeon, G., Legain, D., Durand, P., and Masson, V.: Anthropogenic heat release in an old European agglomeration (Toulouse, France), Int. J. Climatol., 27, 1969–1981, 2007. 4745, 4746, 4753
Pigeon, G., Moscicki, M. A., Voogt, J. A., and Masson, V. 2008: Simulation of fall and winter surface energy balance over a dense urban area using the TEB scheme, Meteorol. Atmos. Phys., 102, 159–171, 2008. 4741, 4745, 4752, 4753

GMDD
8, 4737–4779, 2015

Prusa, J. M., Segal, M., Temeyer, B. R., Gallus, W. A., and Takle, E. S.: Conceptual and scaling evaluation of vehicle traffic thermal effects on snow/ice-covered roads, J. Appl. Meteorol., 41, 1225–1240, 2002. 4739, 4741, 4747

Raatz, W. and Niebrügge, L.: Road weather forecasts for a winter road maintenance information center, in: Proceeding of the 11th SIRWEC Conference, Sapporo, Japan, 6 pp., availabe at http://www.sirwec.org/Papers/sapporo/30.pdf (last access: 17 March 2015), 2002. 4739

Rayer, P. J.: The Meteorological Office forecast road surface temperature model, Meteorol. Mag., 116, 180–191, 1987. 4739

Sass, B. H.: A numerical model for prediction of road surface temperature and ice, J. Appl. Meteorol., 31, 1499–1506, 1992. 4739

Sass, B. H.: A numerical forecasting system for the prediction of slippery roads, J. Appl. Meteorol., 36, 801–817, 1997. 4738

Sailor, D. J. and Lu, L.: A top-down methodology for developing diurnal and seasonal anthropogenic heating profiles for urban areas, Atmos. Environ., 38, 2737–2748, 2004. 4745, 4746, 4753

Shao, J.: A winter road surface temperature model with comparison to others, Unpublished PhD thesis, University of Birmingham, UK, 1990.

Shao, J. and Lister, P. J.: The prediction of road surface state and simulation of the shading effect, Bound.-Lay. Meteorol., 73, 411–419, 1995. 4738

Shao, J. and Lister, P. J.: An automated now casting model of road surface temperature and state for winter road maintenance, J. Appl. Meteorol., 35, 1352–1361, 1996. 4739

Sato, T., Kosugi, K. Abe, O. Mochizuki, S., and Koseki, S.: Wind and air temperature distribution in the wake of a running vehicle, in: Proceeding of the 12th SIRWEC Conference, Bingen, Germany, 7 pp., available at http://www.sirwec.org/Papers/bingen/6.pdf (last access: 22 April 2015), 2004. 4747

Surgue, J. G., Thornes, J. E., and Osborne, R. D.: Thermal mapping of road surface temperatures, Phys. Technol., 13, 212–213, 1983. 4740

Takahashi, N., Asano, M., and Ishikawa, M.: Developing a method to predict road surface icing conditions applying a heat balance method, Proc. Cold Reg. Technol. Conf., 21, 201–208, 2005. 4747

Takle, E. S.: Bridge and roadway frost occurence and prediction by use of an expert system, J. Appl. Meteorol., 29, 727–734, 1990. 4739

GMDD
8, 4737–4779, 2015

Table 1. Dimensions of the vehicle impact zone.

Item	Symbol	Value
Road width	W_{road}	10 m
Vehicle length	L_{veh}	4.5 m
Vehicle width	W_{veh}	1.5 m
Length of the impact area of the engine	L_m	$0.25\,L_{veh}$
Width of the impact area of the engine	W_m	0.8 m
Length of the impact area of the tires	L_p	L_{veh}
Width of the impact area of the tires	W_p	$0.12\,W_{veh}$
Radius of the impact area of the exhaust system	R_{ex}	$0.40\,W_{veh}$

GMDD
8, 4737–4779, 2015

Table 2. Weighing of traffic area impact zones (Khalifa et al., 2014).

Item	Impact area (m^2)	Contribution (%)
Engine	2.025	0.25
Exhaust system	1.765	0.21
Tires	1.800	0.22
Body	2.510	0.32

GMDD
8, 4737–4779, 2015

Table 3. Examples of parameterization of the coatings constituting the built urban area in TEB.

Item		Value	Unit	
Percentage of built area		0.7	(%)	
Buildings height		15	(m)	
Ratio of the width of the canyon and urban buildings height		1.15	–	
Characteristics of the various components of the urban canyon				
		Roof	Road	Walls
Emissivity		0.90	0.94	0.90
Albedo		0.22	0.08	0.20
Number of layer		4	5	4
Layer thickness (m)	1	0.020	0.001	0.010
	2	0.150	0.010	0.040
	3	0.120	0.100	0.015
	4	0.300	0.250	0.060
	5	–	0.600	–
Layer heat capacity ($W K^{-1} m^{-2}$)	1	1 769 000	2 000 000	1 890 000
	2	1 500 000	2 000 000	1 890 000
	3	290 000	2 000 000	804 000
	4	1 520 000	2 000 000	564 000
	5		1 400 000	
Layer thermal conductivity ($W m^{-1} K^{-1}$)	1	0.90	2.00	1.77
	2	0.93	2.00	1.77
	3	0.50	2.00	0.75
	4	0.19	2.00	0.18
	5	–	0.40	–

GMDD
8, 4737–4779, 2015

Table 4. List of abbreviations.

Abbreviations	Synonym	Unit
AC_{road}	Aerodynamic conductance of dry road	–
$AC_{road\text{-}wat}$	Aerodynamic conductance of a wet road	–
AC^{*}_{road}	Aerodynamic conductance's impacted by traffic of dry road	–
$AC^{*}_{road\text{-}wat}$	Aerodynamic conductance's impacted by traffic of wet road	–
C_{ex}	Specific heat of the combustion products	J kg^{-1} K^{-1}
C_{shield}	The shield coefficient	–
C_{turb}	Coefficient of turbulence caused by traffic	–
c_p	Specific heat capacity	J kg^{-1} K^{-1}
d_1, d_2	Thickness of the first and the second layer of the road	m
D_{veh}	Traffic density	vehicles s^{-1}
E_{ex}	Sensible heat flux from the exhaust system	W m^{-2}
FE	Average fuel consumption	km L^{-1}
$FIR_{veh\text{-}inf}$	Downward infrared radiation flux emitted by the lower part of vehicle	W m^{-2}
$FIR_{veh\text{-}sup}$	Upward infrared radiation flux emitted by the upper part of vehicle	W m^{-2}
G	Conductive soil heat flux	W m^{-2}
h	Representative height of urban canyon in the TEB model	m
L	Latent heat flux	W m^{-2}
L^{*}	Latent heat flux impacted by traffic	W m^{-2}
L_v	Latent of liquid water evaporation	J kg^{-1}
L_{veh}	Vehicle length	m
$LW_{Road\_to\_Road}$	Interaction radiative coefficient between road and road	W m−2 K^{-4}
$LW_{Road\_to\_Sun}$	Interaction radiative coefficient between road and sun	W m−2 K^{-4}
$LW_{Snow\_to\_road}$	Interaction radiative coefficient between snow and road	W m−2 K^{-4}
$LW_{Walls\_to\_road}$	Interaction radiative coefficient between walls and road	W m−2 K^{-4}
$LW_{Garden\_to\_road}$	Interaction radiative coefficient between garden and road	W m−2 K^{-4}
m_{ex}	Combustion products mass flow rate	kg s^{-1}
m_{H_2O}	Water vapor mass fraction in the exhaust system	–
NHC	Net heat combustion	J kg^{-1}
Q_{canyon}	Specific air humidity	g kg^{-1}
$Q_{E\_traffic}$	Latent heat flux of traffic	W m^{-2}

GMDD
8, 4737–4779, 2015

Table 4. Continued.

Abbreviations	Synonym	Unit
Q_{E_top}	Latent heat flux of urban canyon	W m^{-2}
$Q_{H\_traffic}$	Sensible heat flux of traffic	W m^{-2}
Q_{H_top}	Sensible heat flux of urban canyon	W m^{-2}
$Q_{traffic}$	Total heat flux generated by traffic	W m^{-2}
Q_{sat_road}	Specific humidity of the road surface	g kg^{-1}
Q_v	Global flux from a vehicle	J s^{-1}
R_n	Net radiation flux	W m^{-2}
R_{nl}	Net long wave radiation at the road surface	W m^{-2}
R^*_{nl}	Net long wave radiation at the road surface impacted by traffic	W m^{-2}
R_{ns}	Net short wave radiation at the road surface	W m^{-2}
R_{ld}	Downward long wave radiation at the road surface	W m^{-2}
R^*_{ld}	Downward long wave radiation at the road surface impacted by traffic	W m^{-2}
R_{lu}	Long wave upward radiation	W m^{-2}
R^*_{lu}	Long wave upward radiation impacted by traffic	W m^{-2}
R_{road}	Aerodynamic resistance of dry road	–
$R_{road\text{-}wat}$	Aerodynamic resistance of a wet road	–
R_{sd}	Downward short wave radiation	W m^{-2}
R_{su}	Upward short wave radiation	W m^{-2}
RST	Road surface temperature	K
RST_2	Temperature of the second layer of road	K
$RST_{With\text{-}traffic}$	RST measured by the IR camera (zone submitted to traffic)	K
$RST_{Without\text{-}traffic}$	RST measured by the IR radiometer (zone not submitted to traffic)	K
$RST_{measured}$	Weighted average of the RST	K
$RST_{TEB\text{-}IC}$	RST simulated according the initial configuration of TEB	K
$RST_{TEB\text{-}A1}$	RST simulated according the first traffic integration approach in TEB	K
$RST_{TEB\text{-}A2}$	RST simulated according the second traffic integration approach in TEB	K
R_v	Radiative heat flux emitted by vehicle	W m^{-2}
S_a	Sensible heat flux	W m^{-2}
S^*_a	Sensible heat flux impacted by traffic	W m^{-2}
S_{impact}	Traffic area impact	m
S_m	Sensible heat flux from the engine	W m^{-2}

GMDD
8, 4737–4779, 2015

Table 4. Continued.

Abbreviations	Synonym	Unit
S_t	Frictional heat flux	W m^{-2}
S_{va}	Vehicle sensible heat due to vehicle-induced wind	W m^{-2}
SVF_{road}	Sky view factor of the road	–
SVF_{walls}	Sky view factor of the walls	–
TEB	Town Energy Balance	–
T_{air}	Ambient air temperature at 2 m height	K
T_{shield}	Time during which the road surface is covered by the vehicle	s
T_{lowcan}	Temperature of the lower limit layer of urban canyon, assimilated to T_{air}	K
t_{time}	Time step	s
T_t	Tire temperature	K
T_v	Shielding time due to only one vehicle	s
T_{veh}	Vehicle temperature	K
$T_{veh\text{-}inf}$	Representative temperature of the lower part of vehicle	K
$T_{veh\text{-}sup}$	Representative temperature of the upper part of vehicle	K
V_{veh}	Vehicle velocity	m s^{-1}
V_w	Natural wind velocity	m s^{-1}
W_{canyon}	Width of the street canyon	m
W_{impact}	Width of the traffic impact area	m
W_{veh}	Width of the vehicle	m
W_{road}	Width of the road	m
Y	Limit of the turbulence zone beyond of the vehicle width	m
Y^*	Normalized distance relative to the width of the vehicle	
$Z_{traffic}$	Impact area of traffic	%
	Greek letters	
α_{comb}	Fraction of water vapor that condenses	–
α_s	Heat transfer coefficient between atmosphere and road surface	W m^{-2} K^{-1}
α_{tp}	Heat transfer coefficient between the tire and road surface	W m^{-2} K^{-1}
ϵ_{garden}	Emissivity of the garden	–
ϵ_{road}	Emissivity of the road	–
ϵ_{snow}	Emissivity of the snow layer	–
ϵ_{veh}	Vehicle emissivity	–
ϵ_{walls}	Emissivity of the walls	–

GMDD
8, 4737–4779, 2015

Table 4. Continued.

Abbreviations	Synonym	Unit
λ_1	Thermal conductivity of the first road layer	W m^{-1} K^{-1}
λ_{fg}	Latent heat of condensation of water vapor	J kg^{-1}
ρ_{air}	Air density	Kg m^{-3}
ρ_{fuel}	Fuel density	kg L^{-1}
$\rho_{road\ croad}$	Volumetric heat capacity	J m^{-3} K^{-1}
σ	Stefan–Boltzmann constant	W m^{-2} K^{-4}
Δ_{Zs}	Thickness of the first layer of the road surface	m
$1/f_{road}$	Fraction of the road relative to the width of urban canyon	–

GMDD
8, 4737–4779, 2015

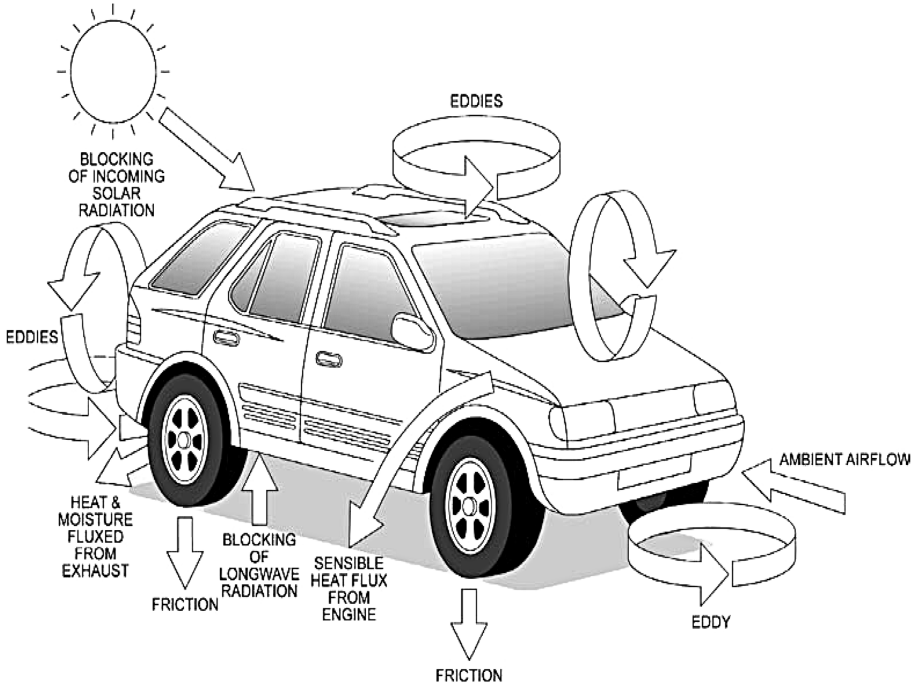

Figure 1. Schematic illustration the impact of traffic on road surface temperature (adapted from Prusa et al., 2002).

GMDD
8, 4737–4779, 2015

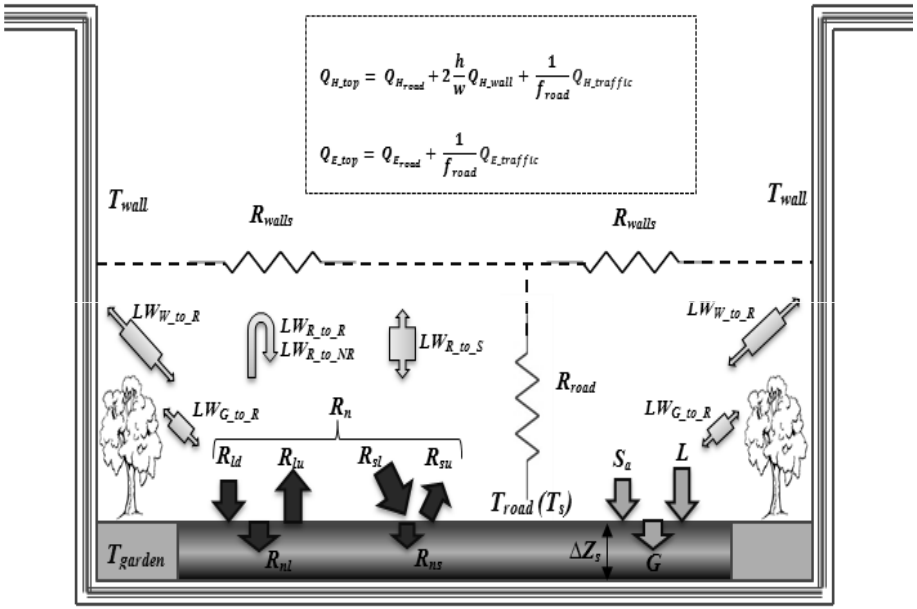

Figure 2. Different physical processes involved in the calculation of road surface energy balance in the initial TEB model configuration.

GMDD
8, 4737–4779, 2015

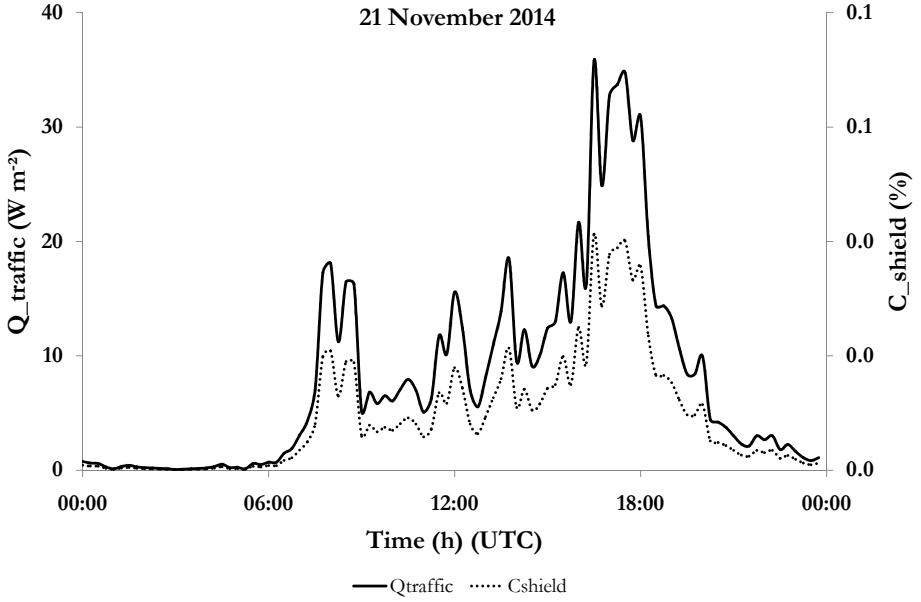

Figure 3. Hourly variations of thermal traffic contributions, and variations of the shield effect coefficient (Rue Charles III, Nancy-France) for the first experiment.

GMDD
8, 4737–4779, 2015

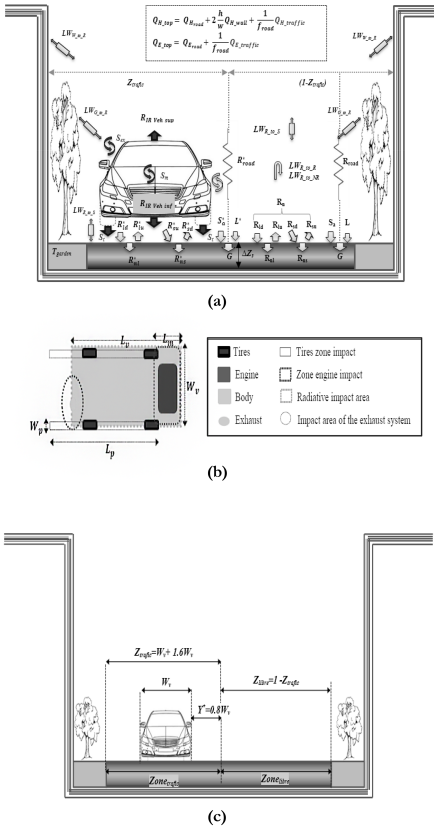

Figure 4. TEB configuration with traffic integration **(a)**, its impact zones of the different processes **(b)** and the limits of the traffic impact zone **(c)**.

GMDD
8, 4737–4779, 2015

Figure 5. Configuration of the street in Nancy (France) for the validation of the two different approaches of traffic implementation in TEB.

GMDD
8, 4737–4779, 2015

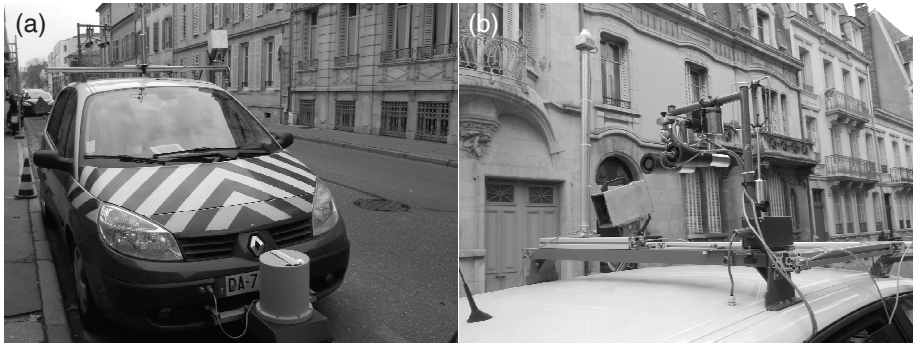

Figure 6. Illustration of car parked in the street with the radiometer on the front bumper **(a)**, and details of instruments installed on the vehicle roof **(b)**.

GMDD
8, 4737–4779, 2015

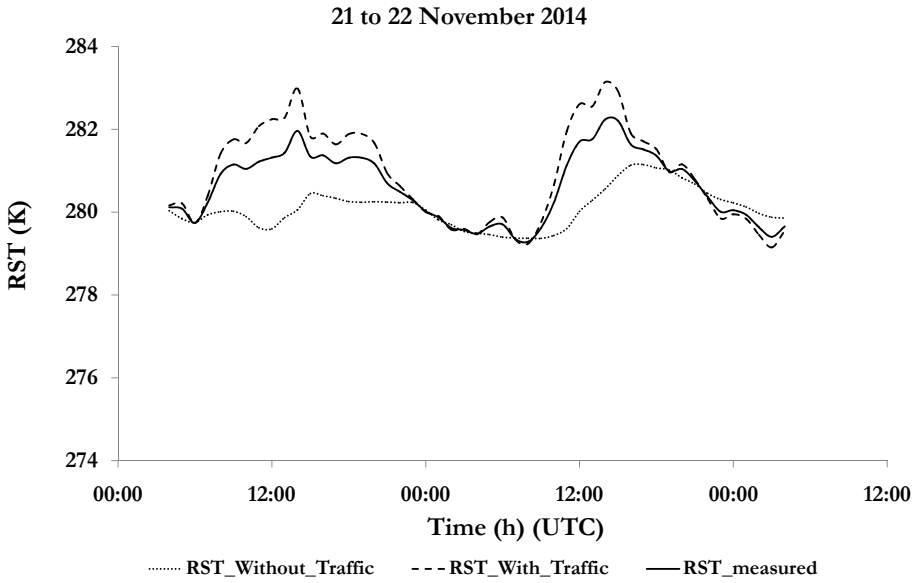

Figure 7. Assessment of the magnitude of traffic impacts on the RST, and illustration of a weighted average temperature of the road surface for the first experiment.

GMDD
8, 4737–4779, 2015

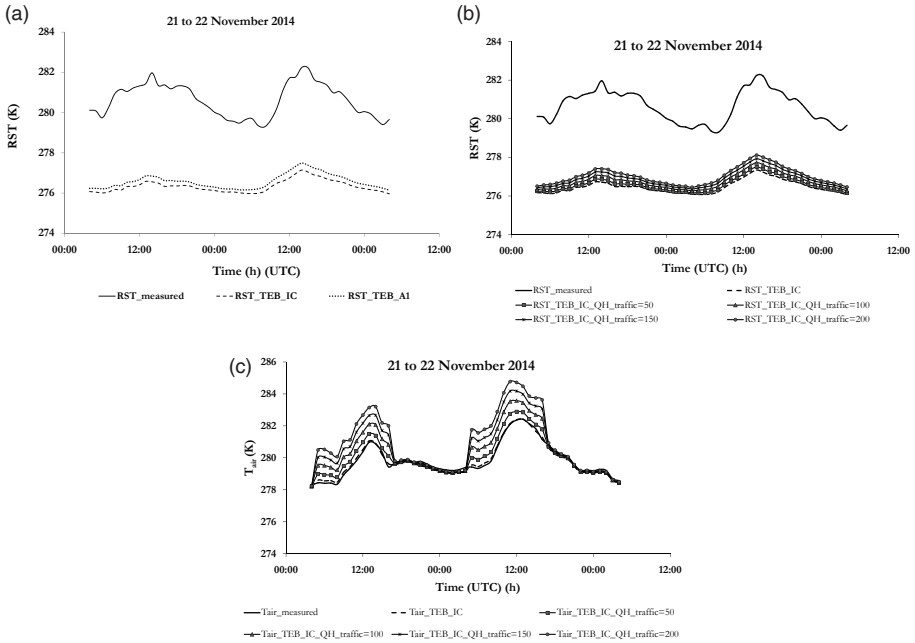

Figure 8. Assessment of the magnitude of traffic impacts on the RST, and illustration of a weighted average temperature of the road surface for the first experiment.

GMDD
8, 4737–4779, 2015

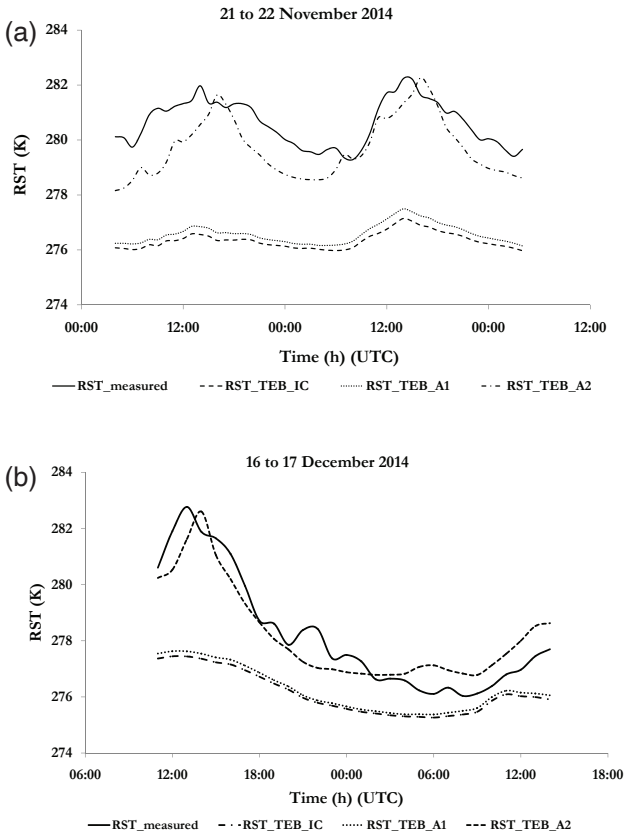

Figure 9. Comparison between RST from TEB in its initial configuration (RST_TEB_IC), RST from TEB via the first approach (RST_TEB_A1), RST from TEB via the second approach (RST_TEB_A2) and field data (RST_measured) for the first **(a)** and for the second **(b)** experiments.

GMDD
8, 4737–4779, 2015

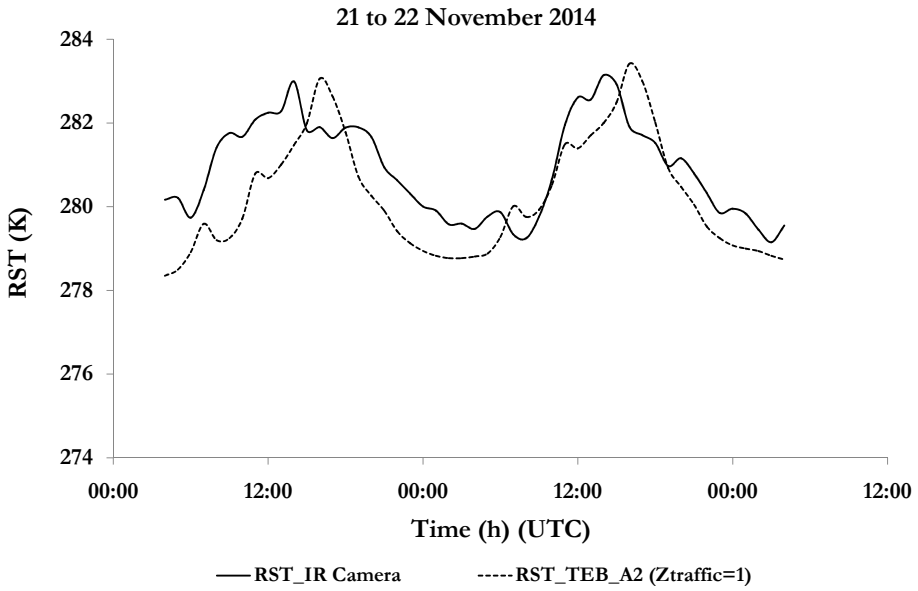

Figure 10. Comparison between RST measured by the IR camera in an area impacted by traffic and RST from TEB via the second approach with Z_{trafic} = 1 for the first experiment.

GMDD
8, 4737–4779, 2015

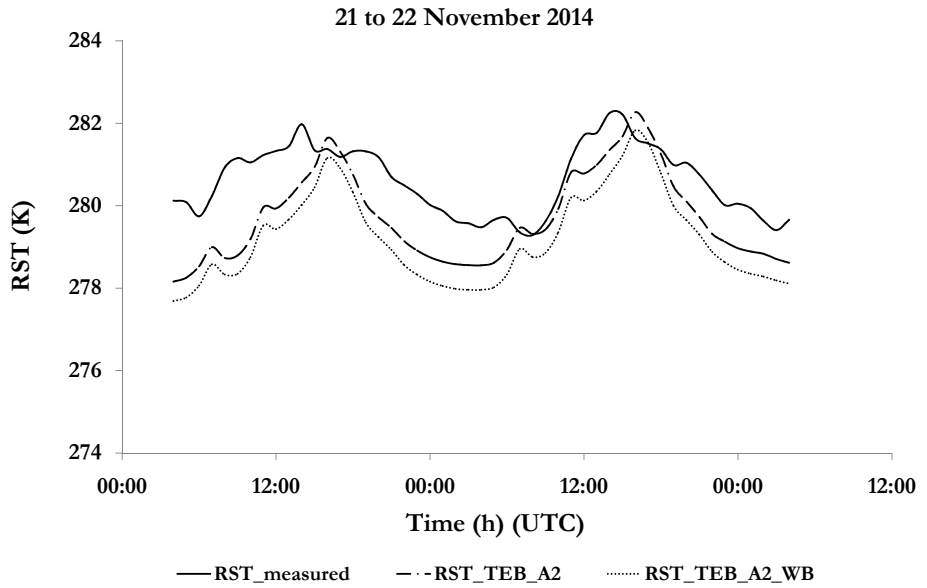

Figure 11. Comparison between RST from TEB via the second approach (RST_TEB_A2), RST from TEB via the second approach without buildings (RST_TEB_A2_WB) and field data (RST_measured) for the first experiment.

GMDD
8, 4737–4779, 2015

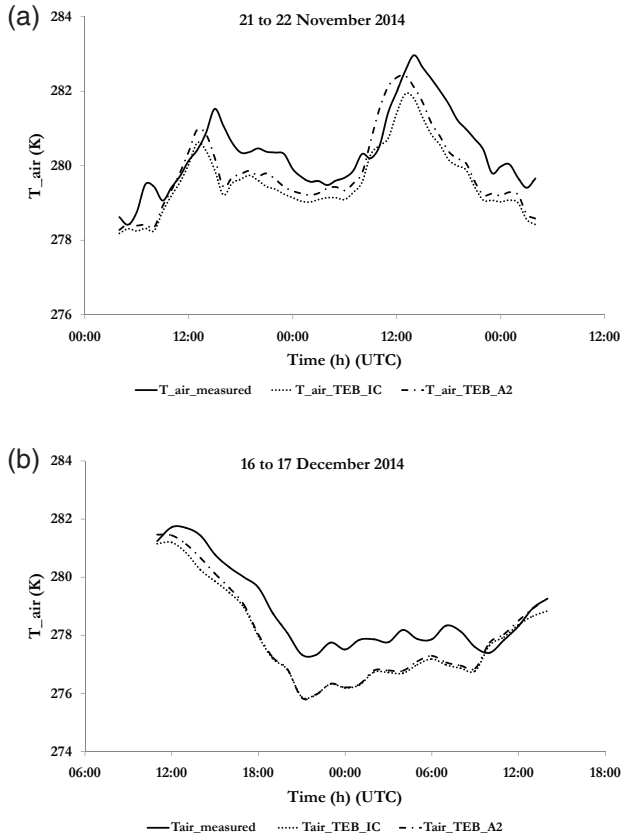

Figure 12. Comparison between air temperature from TEB in its initial configuration (Tair_TEB_IC), air temperature from TEB via the first approach (Tair_TEB_A1), air temperature from TEB via the second approach (Tair_TEB_A2) and air temperature from field data (Tair_measured) for the first **(a)** and for the second **(b)** experiments.

GMDD
8, 4737–4779, 2015